

# Plant Growth Measurement Techniques Using Near-Infrared Imagery

Amr Aboelela     John Barron  
Dept. of Computer Science  
Univ. of Western Ontario  
London, Ontario, Canada, N6A 5B7  
barron@csd.uwo.ca

Albert Liptay  
Agriculture and Agri-food Canada  
Greenhouse and Processing Crop Centre  
Harrow, Ontario, Canada, N0R 1G0  
liptaya@em.agr.ca

**Abstract** We examine the usefulness of various imaging techniques, including optical flow, for measuring plant growth for corn seedlings and Caster Oil Bean leaves. A near-infrared camera, which allows one to measure optical flow in the light and in the dark, is used. For corn seedlings we have already used optical flow to obtain 3D image velocity as a measure of growth performance. We propose two new growth metrics for measuring growth, one based on elongation of the stem/leaf and the other based on the area change of the stem/leaf. These metrics are examined by measuring the corn seedling growth under various combinations of root temperatures (warm or cold) and under various lighting conditions (light to dark). For castor oil bean leaves we use Horn and Schunck's optical flow algorithm to compute the globally consistent flow field for a moving, growing leaf. We use 1<sup>st</sup> order divergence of the flow to hypothesize where growth might be taking place.

**Keywords:** Near-Infrared Imagery, Corn Seedling stem/leaf growth, Caster Oil Bean leaf Growth, Optical Flow, Optical Flow Divergence

## 1 Introduction

We are interested in the measurement of plant growth using optical flow. We use a near infrared-camera with near-infrared light sources, which allows us to measure optical flow in the light and in the dark. Infrared light is just above red light in the visual spectrum and allows us to "see" in the dark with a normal black and white camera with minor modifications. Unlike

infrared light, near-infrared light responds only minimally to heat. Using a near-infrared camera will allow us to measure the growth of corn seedling stems/leaves under various temperature and lighting conditions. We also examine the growth of castor oil bean leaves using a divergence of flow calculation.

## 2 Background

We have presented a non-contact optical method [6] for measuring minute amounts of plant growth using *optical flow* calculations on an image sequence of a sprouting young corn seedling. This method eliminates the plant contact required by use of displacement transducers [9, 10, 11] and the complexity in the setup required when using interferometry [12, 13]. In that study [6], we demonstrated the feasibility of the method for measuring corn seedling growth in 100 images when the corn seedling's root temperature was decreased from about 25° Celsius (room temperature) to about 11° Celsius and then back again to room temperature. Plant growth and root temperature were well correlated (Pearson's coefficient of 0.93); the method could measure growth rates as low as 5 microns/second. In further work [7], much longer image sequences (more than 2000 images) was analyzed by optical flow and the growth not only of an original corn seedling but also (separately) that of leaves emerging from the coleoptile could be measured.

A method was presented to measure 3D plant growth using the optical flow computed on an

image sequence of a growing corn seedling [8]. Each image in the sequence consists of two views of the same growing corn seedling; one view of the corn seedling is front-on while the second view is a orthogonal view (at 90 degrees) of the seedling made by projecting the plant's orthogonal image onto a mirror oriented at 45° with respect to the camera. We compute 3D velocity (motion) of the corn seedling's tip by using a simple extension of the 2D motion constraint equation used in optical flow analysis. We obtain 3D image velocities,  $(v_x, v_y, v_z)$ , in a single least squares calculation.

### 3 Apparatus Description

Our imaging apparatus consisted of a Sony XCEI50 black and white camera with a Schneider Xenoplan 1.4/23mm lens (to allow both visible and near-infrared light to enter the camera) and an RM-90 IR filter (Edmund Optics) in front of the camera's CCD to block out visible light. We used 2 IR LED illumination sources (peak intensity at  $880\text{nm} \pm 25\text{nm}$ ) also made by Edmund Optics. We used a LI-COR-1800 spectroradiometer to measure the spectrum of the near-infrared light sources. Figure 1 shows the measured spectrum for one of our light sources. As can be seen, the spectral irradiance is about 0.85 (watts/m<sup>2</sup>/nm) at 880nm.

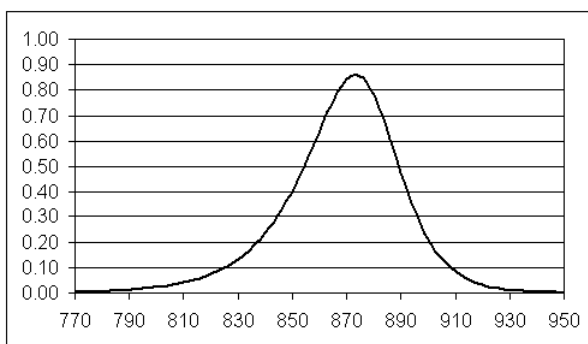


Figure 1: Near-infrared spectrum of the infrared light sources used in our experiment as measured by LI-COR-1800 spectroradiometer.

Corn seeds were sown singly in modified peat moss growing medium in black polyethylene tubes 10 cm long and with a 1 cm inner diameter. The camera, plant/tube and mirror were contained in a wooden box. Figure 2 shows the experimental setup use in our lab.

The use of the box allowed the elimination

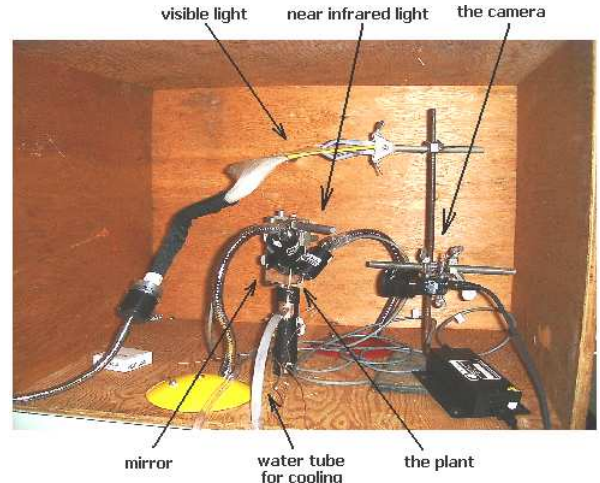


Figure 2: The actual setup

of any room air currents and constant maintenance of the scene temperature and lighting. The tube with a corn seedling at the primary leaf stage was inserted into a glass bottle containing water and coils from water baths set at various temperatures. The seedling shoot was exposed to the ambient room air temperature of about 20°C while the roots in the tube were exposed to the water bath temperature. The seedlings were grown initially at temperatures of 12°C or 24°C for periods of either 100 or 300 minutes. Similarly, a fibre optics light source was turned on or off for either 100 or 300 minute intervals. An image was acquired every 2 minutes during this activity (yielding either 50 or 150 images) for each temperature/lighting period.

Each image in the sequence consists of two views of the same growing corn seedling; one view of the corn seedling is front-on while the second view is a orthogonal side view (at 90 degrees) of the seedling made by projecting the plant's orthogonal image onto a mirror oriented at 45° with respect to the camera. This allows us to measure 3D optical flow by measuring two 2D optical flows [8].

### 4 Optical Flow

We use two optical flow algorithms in the work described here. We use Lucas and Kanade's algorithm [3] extended to give a single 3D image velocity,  $(v_x, v_y, v_z)$ , from front and side views of the same corn seedling. We also use Horn and Schunck's algorithm [4] to measure smooth flow fields on a Castor Oil Bean leaf.

## 4.1 Lucas and Kanade Optical Flow

The basis of all differential optical flow methods is the motion constraint equation,

$$I_x v_x + I_y v_y = -I_t, \quad (1)$$

where  $I_x$ ,  $I_y$  and  $I_t$  are the spatio-temporal image intensity derivatives and  $(v_x, v_y)$  are the  $x$  and  $y$  components of the 2D image motion (image velocity). If the camera is reasonably close to the plane these 2D motions are very good approximations to the actual 3D motions in those dimensions as then perspective projection is roughly orthographic projection. Equation (1) is one equation in two unknowns. Any velocity that satisfies this equation is potentially the correct velocity. If we assume the motion is constant in some neighbourhood then two (or more) sets of derivatives can yield a non-singular linear (least squares) system of equations that yield values for  $(v_x, v_y)$ .

The velocity with the smallest magnitude on the motion constraint equation is called the **normal** velocity as it is one of the endpoints on the shortest line from that point to the origin (this line is perpendicular [normal] to the motion constraint line) and is given by  $\vec{v}_n = v_n \hat{n}$ , where

$$v_n = \frac{-I_t}{\|\nabla I\|_2} \quad \text{and} \quad \hat{n} = \frac{(I_x, I_y)}{\|\nabla I\|_2} \quad (2)$$

are the normal velocity magnitude and the normal velocity direction and  $\nabla I = (I_x, I_y)$  is the spatial intensity gradient. We do not compute or use normal velocities in this study.

Differentiation was done using Simoncelli's [5] matched balanced filters for low pass filtering (blurring) ( $p_5$ ) and high pass filtering (differentiation) ( $d_5$ ) [see Table 1]. Matched filters allow comparisons between the signal and its derivatives as the high pass filter is simply the derivative of the low pass filter and should yield more accurate derivative values. Using these two masks  $I_x$  is computed by applying  $p_5$  in the  $t$  dimension, then  $p_5$  to those results in the  $y$  dimension and finally  $d_5$  to those results in the  $x$  dimension.  $I_y$  and  $I_t$  are computed in a similar manner. Before performing this filtering we use a simple averaging filter  $[\frac{1}{4}, \frac{1}{2}, \frac{1}{4}]$  to slightly blur the images. Simoncelli claims that because both of his filters were derived from the same principles more accurate derivatives result and he demonstrated this on the Yosemite Fly-Through sequence [5, 2]. We use the normal

$n$	$p_5$	$d_5$
0	0.036	-0.108
1	0.249	-0.283
2	0.431	0.0
3	0.249	0.283
4	0.036	0.108

Table 1: Simoncelli's 5-point Matched/Balanced Kernels

motion constraint equation for  $(v_x, v_y)$  given in equation 1 while we use a modified form of the motion constraint equation for the side image

$$-I_x v_z + I_y v_y = -I_t \quad (3)$$

to compute  $(v_y, v_z)$ . Note that the minus sign in front of  $I_x$  is necessary as a negative  $x$  velocity in the front image is a positive  $z$  velocity in the side image. These two equations yield 2 equations in 3 unknowns  $(v_x, v_y, v_z)$ . We measure  $I_x$ ,  $I_y$  and  $I_t$  for the two views and use equations (1) or (3) to set up a linear system of equations which we can solve for in the least squares sense (we must have at least one derivative set from each of the views or a  $(v_x, v_y, v_z)$  calculation is not possible).

## 4.2 Horn and Schunck Optical Flow

Horn and Schunck [4] combined the gradient constraint (1) with a global smoothness term to constrain the estimated velocity field  $\vec{v} = (v_x, v_y)$ , minimizing

$$\int_D (\nabla I \cdot \vec{v} + I_t)^2 + \lambda^2 (\|\nabla v_x\|_2^2 + \|\nabla v_y\|_2^2) dx dy \quad (4)$$

defined over a domain  $D$  (the image), where the magnitude of  $\lambda$  reflects the influence of the smoothness term. We used  $\lambda = 1.0$  and  $\lambda = 10.0$  in this study. Iterative equations are used to minimize (4) and yield the optical flow field as:

$$v_x^{k+1} = \bar{v}_x^k - \frac{I_x [I_x \bar{v}_x^k + I_y \bar{v}_y^k + I_t]}{\alpha^2 + I_x^2 + I_y^2} \quad (5)$$

$$v_y^{k+1} = \bar{v}_y^k - \frac{I_y [I_x \bar{v}_x^k + I_y \bar{v}_y^k + I_t]}{\alpha^2 + I_x^2 + I_y^2},$$

where  $k$  denotes the iteration number,  $v_x^0$  and  $v_y^0$  denote initial velocity estimates which are set to zero, and  $\bar{v}_x^k$  and  $\bar{v}_y^k$  denote neighbourhood averages of  $v_x^k$  and  $v_y^k$ . We use at most 100 iterations in all testing below. Differentiation for computing  $I_x$ ,  $I_y$  and  $I_t$  was done using Simoncelli's filters [5] as outlined above.

### 4.3 Experimental Nomenclature

Our experiments consist of measuring corn seedling growth/motion in a variety of conditions. For example, STEM-LDL-CWC indicates a growth/motion sequence for a stem, with the light/dark condition, LDL, meaning a change in the lighting as Light/Dark/Light every 150 frames. At the same time, CWC means changing the cold/warm condition as Cold/Warm/Cold every 50 frames. At the end of every 150 frames, the CWC sequence repeats itself again but potentially in a different lighting condition, as in this case. The name LEAF-LDL-WCW indicates a growth/motion sequence for a leaf where the light/dark condition, LDL, means a change in the lighting as Light/Dark/Light every 150 frames, while the temperature condition, WCW, means changing the cold/warm condition every 50 frames as Warm/Cold/Warm. At the end of 150 frames the WCW cycle repeats itself. Because each image is acquired at 2 minute intervals, 50 frames equal 100 minutes while 150 frames equal 300 minutes.

### 4.4 Experimental Definitions

For estimating the seedling growth value, in Barron and Liptay's work [6, 7, 8], the image velocities,  $\vec{v} = (v_x, v_y, v_z)$  were summed over time.

Here we introduce a new scalar value called  $V_{norm-total}$  which means to get the total  $L_2$  norm of every single velocity at each frame  $i$ :

$$V_{norm-total} = \sum_{i=1}^n \|\vec{v}_i\|_2. \quad (6)$$

Another scalar value called total displacement ( $D_{total}$ ) is computed as the  $L_2$  norm of the sum of every single velocity vector at each frame:

$$D_{total} = \left\| \sum_{i=1}^n \vec{v}_i \right\|_2. \quad (7)$$

Now, the rate of displacement change,  $D_{rate}$ , is computed as:

$$D_{rate} = D_{total_i} - D_{total_{i-1}}. \quad (8)$$

Here  $i$  denotes the current frame number and  $i - 1$  the previous frame number.

The total elongation of the corn seedling stem/leaf can be approximated by the displacement value based on a sum of velocities. Error in this measure is introduced when the stem/leaf is

bent, then the tip starting point projection position changes with time. Furthermore, because the seedling sometimes just sways about while it is growing, it is inaccurate to measure the  $L_2$  norm of the image velocity components at the corn seedling tip for a short time interval, but rather to measure the displacement over a significant time interval to obtain a better approximation for the seedling elongation. In this way, respective negative and positive values of the  $x$ ,  $y$  and  $z$  components of image velocity will cancel each other out when summed.

### 4.5 Plant Elongation

One way to measure the elongation of the corn seedling involves projecting the tip starting point onto the current growing plant seedling. Figure 3 shows this projection from the tip starting point  $P_{t_1}$  to a projected point  $P_{p_i}$  on the corn seedling at time (current frame)  $i$ .

We determine  $P_{p_i}$  by first getting  $P_{c_i}$  which is the intersection of the lines  $\overline{P_{t_1}P_{f_1}}$  and  $\overline{P_{t_i}P_{f_i}}$  lines, where  $P_{f_1}$  and  $P_{f_i}$  are pixels measured in the bottom row of the corn seedling in frames 1 and  $i$  respectively.

Now  $r$ , the distance from  $P_{c_i}$  to either  $P_{p_i}$  or  $P_{t_1}$  is equal as it is the distance swept along the arc from  $P_{t_1}$  to  $P_{p_i}$ :

$$r = \|P_{t_1}\vec{P}_{c_i}\|_2 = \|P_{p_i}\vec{P}_{c_i}\|_2. \quad (9)$$

Then  $L$ , the stem elongation is:

$$L = \|P_{t_i}\vec{P}_{c_i}\|_2 - \|P_{p_i}\vec{P}_{c_i}\|_2. \quad (10)$$

Given the intersection point of lines  $\overline{P_{t_1}P_{f_1}}$  and  $\overline{P_{t_i}P_{f_i}}$ , i.e.  $P_{c_i}$ , we can compute the projection point  $P_{p_i}$  as the point on the ray given by:

$$P_{p_i} = P_{c_i} + \frac{\overline{P_{c_i}P_{t_i}}}{\|P_{c_i}P_{t_i}\|_2} * r. \quad (11)$$

In the event that "bends" appear in the stem, if those bend points can be detected, then this elongation method can easily be extended to handle them.

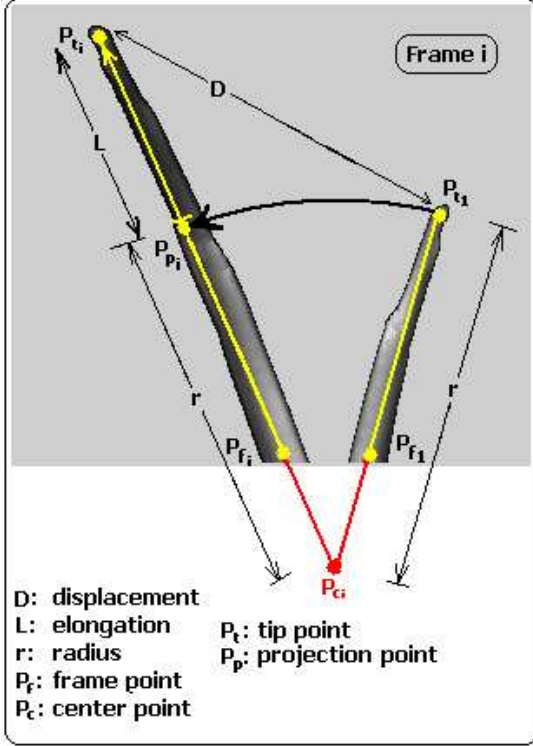


Figure 3: Measuring the corn seedling elongation as the stem sways: we want to measure elongation of the stem only.

#### 4.6 Plant Area Change

A second way to measure corn seedling growth is to measure the area extension of the plant from frame 1 to frame  $i$ , as shown in Figure 4. As in the previous section, we compute  $P_{p_i}$ , the projection of  $P_{t_i}$  onto the line  $\overline{P_{c_i}P_{t_i}}$ . From that point (upwards) we compute whether a pixel belongs to a plant stem or the background by a simple threshold on grayvalue (30). A simple count of these stem pixels gives a rough estimate of area increase. Note here that we are assuming that the stem areas below  $P_{t_i}$  and  $P_{p_i}$  are equal; actually the area under  $P_{p_i}$  will probably be a bit bigger because of subsequent growth.

For a corn seedling stem/leaf we can also count the number of pixels comprising its surface. This involves use a threshold  $\tau$  (we use value 30) to separate background pixels from stem/leaf pixels. The total area then represents the total growth:

$$A_{total} = Count(P(i, j)), \text{ such that } P(i, j) \geq \tau,$$

where  $P(i, j)$  is the pixel at location  $(i, j)$ . Also, the  $P(i, j)$  pixels should be above the  $P_{p_i}$  (Pro-

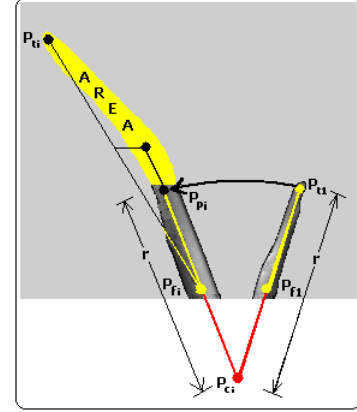


Figure 4: Another way to measure the growth by computing the area extension of the corn seedling.

jection Point) position to be counted in the area computations as shown in Figure 4.

The initial value for  $\tau$  is 10.0 then we change it when the lighting condition changes because at that time the plant pixel intensities would change also and would give a rise or a decrease in the total computed area, so to compensate that change, we tune the value  $\tau$  by decreasing or increasing it, to cancel out the light intensity change affection. We use a binary search method to get the best new  $\tau$  to cancel out the intensity effect. This mostly happens in frame number 150 and 300 when the light condition change from dark to light and vice versa.

The rate of area change can be specified as:

$$A_{rate} = A_{total_i} - A_{total_{i-1}}.$$

## 5 Experimental Results

Figure 5 shows the result of LEAF-LDL experiment when we measure the area (Figure 5a) and when we measure the elongation (Figure 5b). In Figure 5a the white coloured pixels are those with grayvalue over threshold  $\tau \geq 30$ . In Figure 5b we see several things: the jagged lines show the path of the seedling tip as it grows, the straight lines are the displacement vectors,  $D_{total}$ , the straight horizontal lines mark 50 image intervals and the curved arc-like lines are the paths of the projections of  $P_{f_i}$  in the front and side views to  $P_{p_i}$  in those views.

Figure 6 shows the elongation rate,  $L_{rate}$ , and the total elongation,  $L_{total}$ , of LEAF-LDL experiment, as a function of the frame number. Fig-

Figure 7 shows the area rate,  $A_{rate}$ , and the total area,  $A_{total}$ , as a function of the frame number.

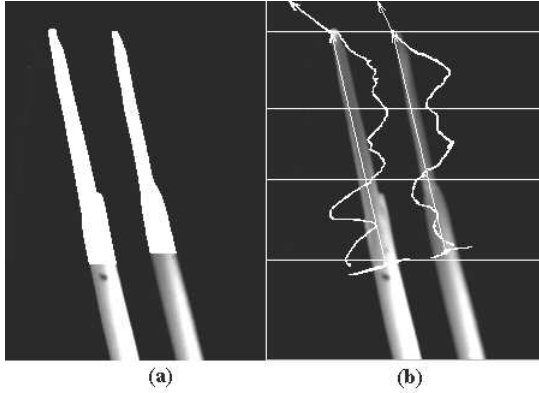


Figure 5: LEAF-LDL experiment where we show how we measure (a) the area and (b) the elongation.

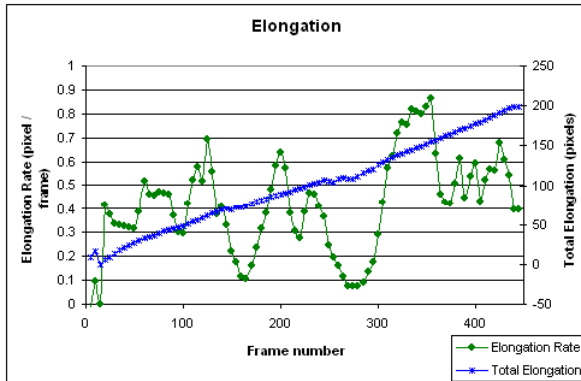


Figure 6: Elongation rate and total elongation for the LEAF-LDL experiment measured as a function of frame number.

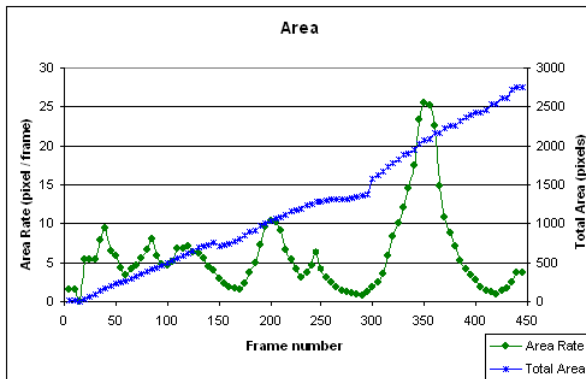


Figure 7: Area rate and total area for the LEAF-LDL experiment measured as a function of the frame number.

Figure 8 shows normalized elongation rate and area rate, computed by dividing the original rates measures by the rate averages over the total frame period (450 frames). This makes the two measures have the same minimums and maximums and allows comparison. The two measures are very similar, Pearson's Correlation Coefficient is 0.66

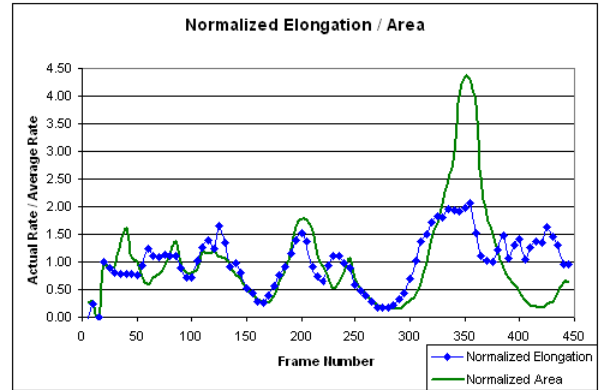


Figure 8: LEAF-LDL experiment showing normalized elongation and area rate,  $L_{rate}$  and  $A_{rate}$ . Pearson's Correlation Coefficient is 0.66.

## 5.1 Corn Seedling Leaf Growth

Corn seedling stem and leaf growth do not seem that different, although a leaf appears to grow much faster in the light than the dark. Figure 9 shows the growth paths for a leaf totally in the light and totally in the dark while Figure 10 shows the growth paths for a leaf in DLD and LDL lighting conditions. The leaf in the fully lighted scene is drawn to the light source. LDL or DLD lighting conditions seem to have little effect, as for the stem.

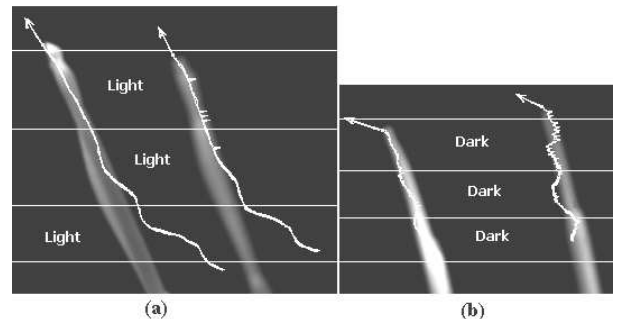


Figure 9: The growth of a leaf in light and in dark.

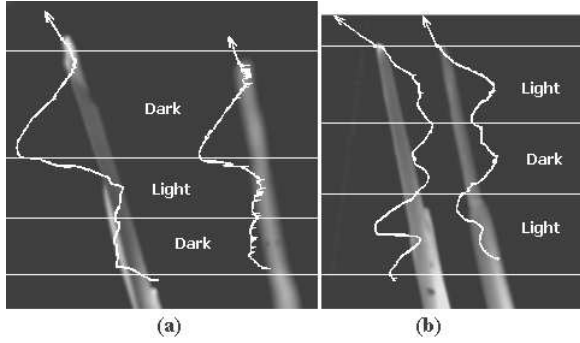


Figure 10: The growth of a leaf in a DLD or LDL sequence.

## 5.2 Overall Statistics

Figure 11 shows the average growth for all our experiments in the warm or in the cold (or some combination of these) for all lighting conditions. The darks parts (purple) at the top of the pole are the standard deviations while the lighter parts (cyan) represent the average values. Figure 12 shows the average growth for all out

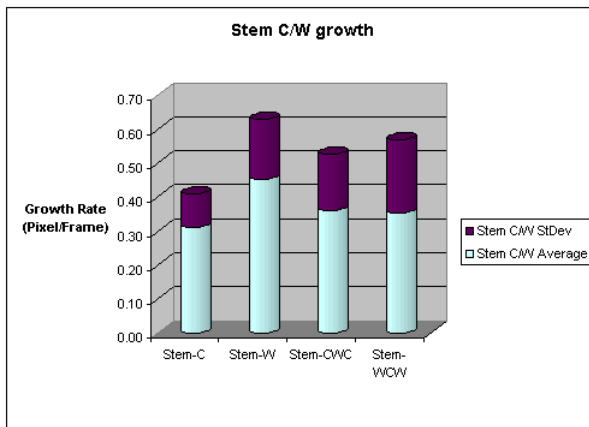


Figure 11: Average stem growth rate according as a function of root temperature, C, W, CWC or WCW.

experiments in the light and in the dark (or some combination of these) for all root temperatures. These experiments show that the rate of growth is fastest for warm root temperatures, slowest for the cold root temperatures and in-between and about the same for the CWC and WCW sequences. Lighted stems grow faster than dark stems and when the lighting is mixed the growth rate is in-between; LDL sequences show slightly more growth than DLD sequences (which makes

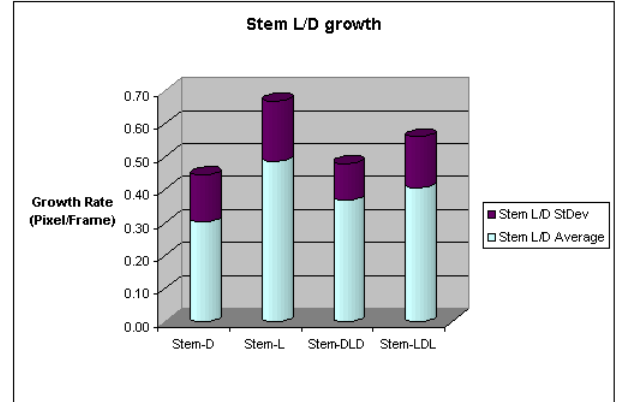


Figure 12: Stem growth rate according to the change in dark/light conditions.

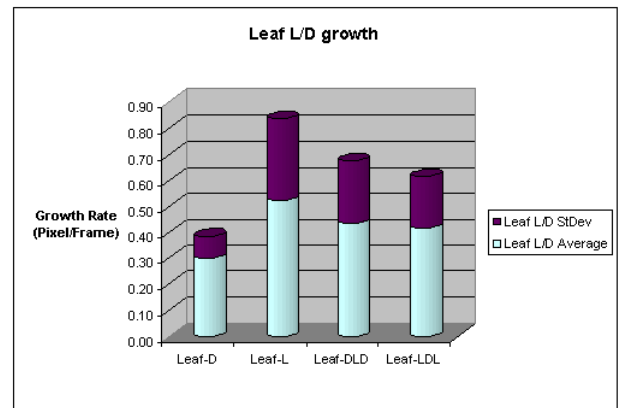


Figure 13: Leaf growth rate according to the change in dark/light conditions.

sense as they are exposed to more light).

Corn seedling leaf overall growth statistics are not much different than those for a corn seedling stem. Figure 13 shows this.

## 5.3 Castor Oil Bean Leaf Growth

In this section we examine the divergence of optical flow as a means to measure leaf growth. Figure 14 shows an image of a Castor oil bean leaf. This leaf is moving as it grows and we verified that the leaf moves with the computed flow. Jähne et al. [14] also investigated the use of optical flow to measure motion in dynamic processes, like castor oil bean leaf growth via divergence. They used a 2 frame calibration technique to correct for camera defects. Nevertheless, we obtained similar results to them using our near-infrared camera. We first tried to measure optical flow using Lucas and Kanade's least

squares method [3] but we found the flows too sparse. We report Horn and Schunck’s method [4] with the Lagrange multiplier  $\alpha$  set to 10 and using 100 iterations. Figure 15 which shows the flow for frame number 100 from the 450 frames sequence.

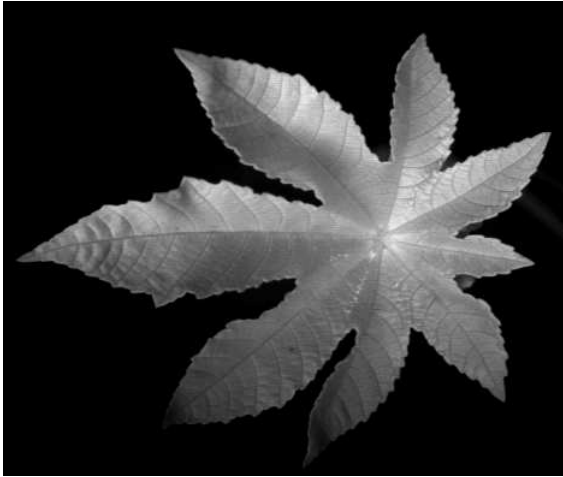


Figure 14: An image of the Castor Oil leaf in frame number 100.

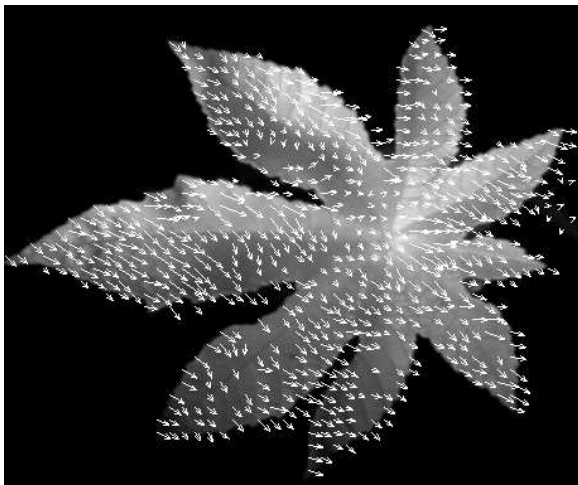


Figure 15: Horn and Schunck result using  $\alpha = 10$ . This one is for frame 100.

We compute the image velocity divergence as:

$$Divergence = \sqrt{\left(\frac{\partial v_x}{\partial x}\right)^2 + \left(\frac{\partial v_y}{\partial y}\right)^2}.$$

$\left(\frac{\partial v_x}{\partial x}, \frac{\partial v_y}{\partial y}\right)$  are computed using Simoncelli’s filters on the  $(v_x, v_y)$  computed via the Horn and Schunck iterations. Like Jähne et al. [14] we hypothesize that high absolute values of

*Divergence* correspond to positions of growth (but we have no way of verifying this at the present). Figure 16 shows the divergence image. The black spots indicate high divergence and made indicate leaf growth.

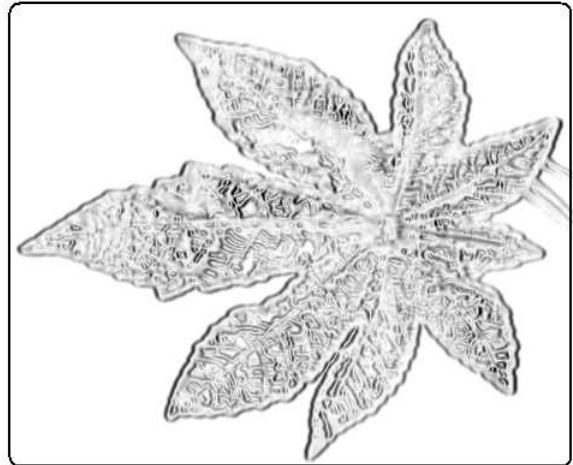


Figure 16: The *Divergence* image for frame 100.

## 6 Conclusions and Future Work

We have shown a number of metrics that may be a useful measuring tool for plant growth. Stem/leaf elongation seems to be good metrics for corn seedling growth. Corn Seedling stems/leaves seem to grow faster when their root temperature is warmer or when they are exposed to more light. These expected results are confirmed by our growth measurements. Lastly, we hypothesized that the divergence of an optical flow field of a moving/growing leaf might be a means of measuring leaf growth.

Future work includes, using longer time sequences (simulating a day which is warm in the light and colder in the dark), using “older” plants where lighting conditions would produce more pronounced growth effects, measuring leaf growth and correlating this to surface area growth and measuring divergence on plants with many overlapping leaves.

**Acknowledgements:** We thank Nick Dimenna for his technical assistance. This work was supported in part by NSERC (Natural Sciences and Engineering Research Council of Canada) through an equipment and an operating grant and by Agriculture and Agri-Food Canada. This

paper is essentially the same as the one with the same title that appeared in the Vision Interface conference, held in Halifax, Nova Scotia in 2003, pp27-34.

## References

- [1] A. Aboelela (2002), "Near-Infrared Optical Flow for Plant Growth", MSc Thesis, Dept. of Computer Science, The University of Western Ontario.
- [2] J. L. Barron, D. J. Fleet and S. S. Beauchemin. Performance of optical flow techniques. *Int. Journal of Computer Vision*, **12(1)**, 1994, pp. 43–77.
- [3] B. D. Lucas and T. Kanade. An iterative image-registration technique with an application to stereo vision. *DARPA Image Understanding Workshop*, 1981, pp. 121–130 (SEE also *IJCAI'81*, pp. 674-679).
- [4] B. K. P. Horn and B. G. Schunck (1981), "Determining optical flow", *Artificial Intelligence (AI)*, vol. 17, pp185-204.
- [5] E.P. Simoncelli, "Design of multi-dimensional derivative filters", *IEEE Int. Conf. Image Processing*, Vol. 1, pp. 790-793, 1994
- [6] Barron, J.L. and A. Liptay (1994) Optical flow to measure minute increments in plant growth. *Bioimaging*, 2:1, pp57-61.
- [7] Liptay A., Barron J.L. , Jewett T. and Wesenbeeck I. van (1995), Oscillations in corn seedling growth as measured by optical flow, *J. Amer. Soc. Hort. Sci.* 120:3, pp379-385.
- [8] Barron, J.L. and A. Liptay (1997) Measuring 3D plant growth using optical flow. *BioImaging* 5, pp82-86.
- [9] Lang A. (1990) Xylem, phloem and transpiration flows in developing apple fruits, *J. Exper. Bot.* 41, 645-651
- [10] Luthen H., Bigdon M. and Bottger M. (1990) Reexamination of the acid growth theory of auxin action, *Plant Physiol.* pp931-939
- [11] Pasumarty S.V., Minchin P.E.H., Fountain D.W. and R.G. Thomas (1991) Influence of shade on the growth and sink activity of young flower heads and peduncles of white clover (*trifolium repens* L.), *J. Exp. Bot.* 42, pp705-710
- [12] Fox M.D. and L.G. Puffer (1976) Analysis of transient plant movements by holographic interferometry. *Nature* 261, June pp488-490
- [13] Jiang Z. and W. Staude (1989) An interferometric method for plant growth measurements. *J. Exp. Bot.* 40, pp1169-1173
- [14] Jähne B., Haußecker H., Scharr H., Spies H., Schmundt D. and U. Schurr, "Study of Dynamical Processes with Tensor-Based Spatiotemporal Image Processing Techniques", *ECCV98*, Vol. 2, Springer-Verlag, LNCS 1407, pp322-335.

## Amr Aboelela

Amr Aboelela was born in Alexandria, Egypt. He obtained his B.Sc. in 1996 in Computer Science from the Department of Computer Science and Automatic Control, Faculty of Engineering, Alexandria University, Egypt. He obtained his M.Sc. from the Department of Computer Science from the University of Western Ontario in 2003. He has worked in the fields Database, Systems and Web Programming in Egypt, Saudi Arabia, Canada and the United States. Currently he is a Software Designer doing Internet Applications.



## Albert Liptay

Albert Liptay was born near Toronto, Ontario, Canada and studied Horticulture for his B.Sc. and M.Sc. degrees at the University of Guelph and obtained his Ph.D. in Cell and Molecular Biology from McMaster University. He was a research scientist at the Federal Government Department of Agriculture (Agriculture and Agri-Food) for 29 years. In 2003 he joined Stoller Enterprises Inc. in Houston, Texas as Director of Research and Development. He is very interested in the use of digital imaging in plant evaluation for crop productivity, real time plant growth extension and non-invasive methods of analysing plant growth and development.



## John Leonard Barron

John Barron was born in Corner Brook, Newfoundland, Canada. He obtained 1<sup>st</sup> class honours B.Sc and B.A degrees in Physics and Computer Science in 1978 from Memorial University and his M.Sc. and Ph.D degrees in Computer Science from the University of Toronto in 1980 and 1988 respectively. Currently, he is a professor of Computer Science at the University of Western Ontario. His main research interests include 2D/3D optical flow, 3D range flow, the recovery of camera motion and scene structure from optical flow, storm detection and tracking on 3D Doppler radar images and the measurement of plant growth using 2D/3D optical flow and 3D range flow.

